ELSEVIER

Contents lists available at ScienceDirect

Separation and Purification Technology

journal homepage: www.elsevier.com/locate/seppur



Enhanced desalination efficiency in capacitive deionization with an ion-selective membrane

Yu-Jin Kim, Jae-Hwan Choi*

Department of Chemical Engineering, Kongju National University, 275 Budae-dong, Seobuk-gu, Cheonan, Chungnam, 331-717, South Korea

ARTICLE INFO

Article history:
Received 6 July 2009
Received in revised form 30 October 2009
Accepted 30 October 2009

Keywords: Capacitive deionization Ion-selective membrane Carbon electrode Electric double layer Current efficiency

ABSTRACT

In order to investigate ionic adsorption and desorption mechanisms on carbon electrode surfaces, capacitive deionization experiments were carried out with two types of capacitive deionization (CDI) cell configurations. A CDI cell equipped with carbon electrodes only and a membrane capacitive deionization (MCDI) cell having a cation-exchange membrane on the cathode surface were constructed, and desalination experiments were carried out at various operating conditions. The conductivity transients of effluents and currents passed through the cells were accurately measured by a potentiostat in order to analyze the transport mechanism at the carbon electrode surfaces. The salt removal efficiencies of the MCDI cell were enhanced by 32.8–55.9% compared to the CDI cell, depending on the operating conditions. Furthermore, the current efficiencies were improved for the MCDI cell: 83.9–91.3% versus 35.5–43.1% for the CDI cell. It was verified that ions were selectively transported between the electric double layer at the electrode surface and the bulk solution in the MCDI cell configuration when a potential was applied. On the contrary, in the case of the CDI cell, both anions and cations were transported during the sorption and desorption processes, which led to decreased salt removal and current efficiencies.

© 2009 Elsevier B.V. All rights reserved.

1. Introduction

Desalination process such as evaporation, ion exchange, reverse osmosis (RO), and electrodialysis (ED) are generally applied to separate ionic substances from aqueous solution [1,2]. These processes all have various advantages and disadvantages; the equipment for the evaporation process is very simple and allows for high-purity fresh water to be obtained, but the energy cost is very high. In the ion-exchange process, a highly concentrated salt brine waste is generated during the regeneration of the resins; also, in RO and ED processes, it is difficult to maintain a constant permeate flux due to membrane fouling and scaling problems [1,3–5]. Concerns about environmental and energy problems have increased over recent years from a global viewpoint. As a promising answer to these problems in the area of desalination technology, many studies have been performed on capacitive deionization (CDI) [6–12].

The CDI process is defined as a potential-induced adsorption of ions onto the surface of a charged electrode. When an electrical potential was applied to the electrode, charged ions migrate to the electrode and are held in the electric double layer (EDL); once the potential is removed, adsorbed ions are quickly released back to the bulk solution [13]. It is known that CDI is an energy-efficient desali-

nation process because it operates at a lower electrode potential (about 1–2 V) at which no electrolysis reactions occur. In addition, this process is environmentally friendly because it requires no chemicals during the operation [13,14].

Because the CDI process uses an adsorption reaction on the electrode surface, it is very important to increase the specific capacitance of the electrode itself. Accordingly, many studies have been conducted to manufacture an electrode for the CDI process from activated carbon cloth [12], carbon felt [15], carbon nanotubes [16,17], and carbon aerogels [6–8,13,18]. In addition, previous researches demonstrated that the capacitance is also dependent upon the surface properties of electrodes such as surface area, pore microstructure and size distribution [13,19–21], chemical functional groups [22], and adsorption properties [23].

However, the salt removal efficiency may show large differences even for the same electrode, depending on the adsorption and desorption mechanism at the EDL. Conventional CDI is known to be energy inefficient because of the dissolved salt present in the pore volume of the carbon electrode [24]. When an electric potential is applied, counter-ions in the pore adsorb onto the electrode and co-ions are expelled from the electrodes. This means that ion adsorption and desorption occur simultaneously on the electrode, which will seriously reduce desalination efficiency.

To solve these problems, Lee et al. [25] introduced a membrane capacitive deionization (MCDI) system in which ion-exchange membranes were incorporated along with the electrodes and developed an MCDI system to test desalination performance

 ^{*} Corresponding author. Tel.: +82 41 521 9362; fax: +82 41 554 2640.
 E-mail address: jhchoi@kongju.ac.kr (J.-H. Choi).

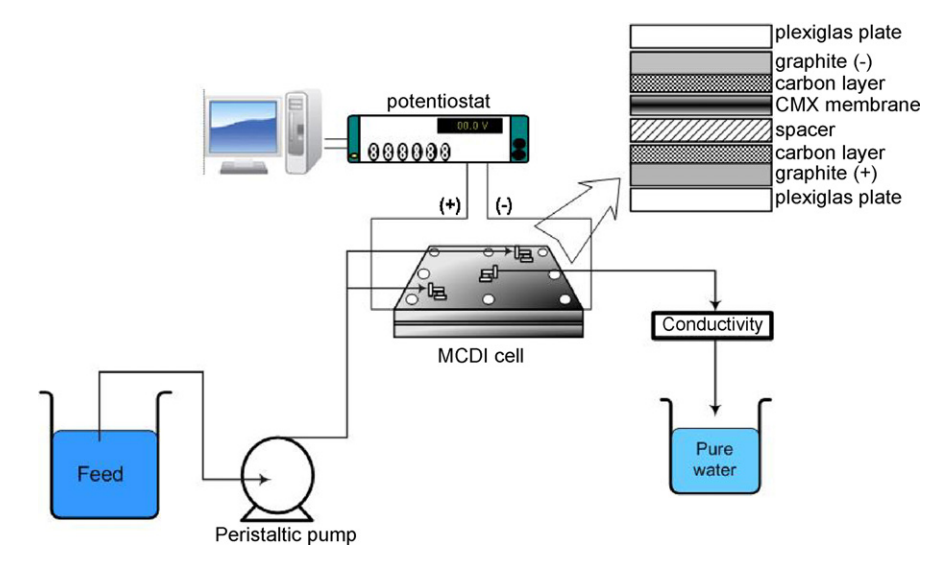


Fig. 1. Schematic diagram of capacitive deionization experiments.

in power plant wastewater. According to their results, the salt removal efficiency by MCDI was 19% higher than that by standard CDI. Li et al. [17] have constructed a novel MCDI device using carbon nanotube and nanofiber electrodes and ion-exchange membranes. They have shown that salt removal by the MCDI system was 49.2% higher than that by the CDI system. From these works, it has been verified that an MCDI system can increase desalination efficiency significantly compared to the CDI system, but the specific mechanism of ion transport in the MCDI system was not yet explained.

In this study, we examined the ion-transport mechanisms in an MCDI system during the sorption and desorption periods. For this purpose, we fabricated carbon electrodes and constructed two cells using these electrodes: CDI and MCDI cells. Several desalination experiments were conducted at various operating conditions, and the conductivities of effluents and currents passed through the cells were accurately measured by potentiostat to elucidate the ion-transport mechanism in the MCDI system.

2. Experimental

2.1. Fabrication and characterization of carbon electrodes

To fabricate the carbon electrodes, a carbon slurry was prepared as a suspension of activated carbon powder (P-60, Daedong AC Corp., specific surface area = $1260\,\mathrm{m}^2/\mathrm{g}$) and poly(vinylidene fluoride) (PVdF, M.W. = 275,000, Aldrich) in di-methylacetamide (DMAc, Aldrich). The mixture was stirred for 12 h to ensure homogeneity. The slurry was then cast onto a graphite sheet (F02511, Dongbang Carbon Corp., Korea) to a thickness of $300\,\mu\mathrm{m}$. The coated electrode was dried at $50\,^{\circ}\mathrm{C}$ in an oven for 2 h and then in a vacuum oven at $50\,^{\circ}\mathrm{C}$ for 2 h to remove all organic solvents remaining in the micropores of the electrode. After the electrode was dried, the weight was measured to determine the amount of carbon coated onto the graphite sheet.

To examine the electrochemical properties of the prepared carbon electrodes, electrical impedance spectroscopy (EIS) measurements were made using a three-electrode system. The carbon electrode specimen was inserted into the specimen holder with an exposed apparent surface area of 1.77 cm². A platinum net and a saturated Ag/AgCl electrode were used as the counter and reference electrodes, respectively. The electrolyte solution used was 0.5 M KCl. All experiments were maintained in a water bath at 25 \pm 0.1 °C.

To examine the internal resistance of the electrodes and their capacitance according to frequency, impedance measurements were performed with an AutoLab PGST30 potentiostat combined with a FRA impedance analyzer. The impedance spectra were obtained at a potential of 0.0 V vs. saturated Ag/AgCl in the frequency range of 100 Hz to 20 mHz. An alternating sinusoidal signal of 25 mV peak-to-peak was superimposed on the DC potential.

2.2. Capacitive deionization experiments

Capacitive deionization experiments were carried out in a flow-through system, depicted in Fig. 1. The system consisted of a reservoir, a peristaltic pump, a CDI unit cell, and a conductivity meter. The CDI unit cell consisted of two parallel porous carbon electrode sheets separated by a non-electrically conductive spacer (nylon cloth, $100\,\mu m$ thick). This prevented an electrical short and allowed liquid to flow. The size of a carbon electrode was $100\,m m \times 100\,m m$. The weight of carbon powder coated on the electrode was 1.3 g. Graphite sheets were used as inert current collectors on the backside of the carbon electrodes. A Plexiglas plate was used to assemble the upper and lower parts of the unit cell.

To examine the effect of the ion-exchange membrane on the desalination efficiency, another CDI cell was constructed with an ion-exchange membrane. In this cell (MCDI), the cation-exchange membrane (Neosepta CMX, Tokuyama Soda Corp.) was inserted between the cathode carbon electrode and spacer. Thus, the assembly of the unit cell is in this order: plate/graphite sheet/anode electrode/nylon spacer/CMX membrane/cathode electrode/graphite sheet/plate.

The capacitive deionization experiments were conducted to compare the salt removal efficiency for the two cell configurations (CDI and MCDI) of the manufactured electrode. A flow channel was created by punching a 1-cm-diameter hole in the center of the electrode so that the solution could be in contact with all sides of the electrode and could run through a spacer to the central hole. NaCl solution (200 mg/L) was supplied to the cell using a peristaltic pump.

A given potential was applied to the CDI cell using a potentio-stat (WPG100, WonA Tech Corp.). We first conducted an adsorption test while applying an already established potential for 3 min, and then we conducted a desorption test immediately afterward for 2 min by changing the electrode potential to 0 V. The conductivity of the effluent water that passed through the cell was measured by connecting a conductivity meter to the position where the solution was released. The conductivity was automatically measured at 1.0-s intervals by connecting the conductivity meter to a data acqui-

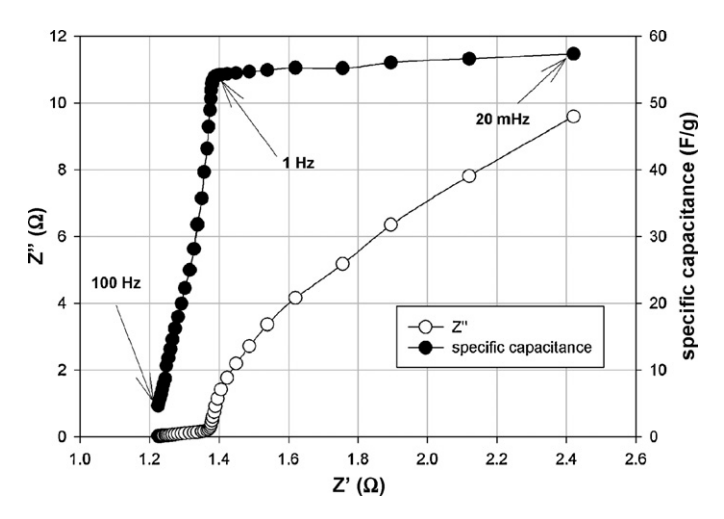


Fig. 2. Complex plane (Nyquist) plot and the *R*–*C* plot (capacitance vs. real part of the impedance *Z'*) on the prepared carbon electrode.

sition system (midi Logger GL200, GraphTech). The CDI tests were conducted at 1.2 and 1.5 V potentials to compare the salt removal efficiency at these values. The effects of changes in the flowrate were examined by supplying 20 or 30 mL/min of solution at 1.5 V.

3. Results and discussion

3.1. Electrochemical properties of the prepared carbon electrode

It has been known that the best method to measure double-layer capacitance is to analyze electrochemical impedance spectroscopy measurements. A complex plane plot (or Nyquist plot) for the impedance response obtained from the prepared carbon electrode is shown in Fig. 2. Two distinct regions appear in the plot for 100 Hz to 20 mHz. This can be explained by the propagation of the AC signal into the pores of the carbon electrode. According to the theoretical analysis on the impedance spectroscopy of porous carbon electrode, the AC signal is increasingly propagating into the inner pore sites of the electrode with decreasing frequencies [26–28]. This revealed the charging characteristics of the carbon electrode.

Specific capacitance (C) can be derived from the imaginary part (Z'') of the impedance spectrum according to [27]:

$$C = \left| \frac{1}{\omega Z''} \right| \tag{1}$$

where ω denotes the angular frequency of the applied AC signal. The corresponding plot of capacitance versus the real part of the impedance is shown in Fig. 2.

Capacitances increased steeply with decreasing frequency up to about 1 Hz. The AC signal can charge more inner surface sites of the carbon electrode with decreasing frequency, resulting in a higher capacitance. At lower frequencies below 0.2 Hz, the total surface of the carbon seems to be covered, so that the capacitance remained at an almost constant value [26]. As shown in Fig. 2, specific capacitance of the carbon electrode prepared in this study was determined to be about 56 F/g in 0.5 M KCl solution.

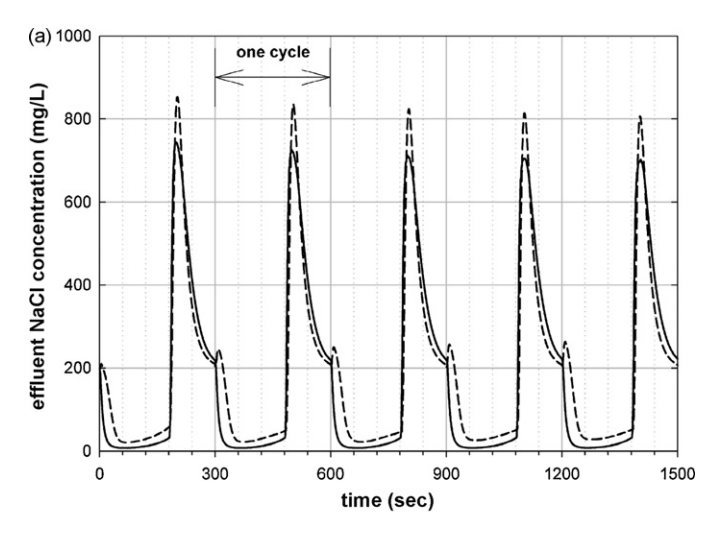
3.2. Comparison of effluent concentrations for the CDI and MCDI cell operations

Desalination experiments for CDI and MCDI cells were performed at a flowrate of $20\,\text{mL/min}$. After applying an adsorption potential of $1.5\,\text{V}$ for $3\,\text{min}$, the electrode potential was immediately changed to $0.0\,\text{V}$ for $2\,\text{min}$. Fig. 3(a) shows the NaCl concentration transients of the effluent for each cell configuration. The NaCl con-

centration was determined from the linear relationship between NaCl concentration and conductivity. The concentration changes show reproducible results for all cycles of sorption and desorption. In order to observe the adsorption and desorption behavior the concentration changes in the second cycle are depicted in Fig. 3(b). When the adsorption potential was applied ions were quickly adsorbed, so that the effluent concentration decreased with time rapidly from the initial 200 mg/L to a minimum of 20.5 mg/L, and to 7.1 mg/L for the CDI and MCDI cells, respectively. Due to the limited ion adsorption capacity of the electrode the number of ions that are adsorbed to the electrode surface gradually decreases. Accordingly, the concentration increased slowly after the minimum point during the adsorption period.

Regarding the desorption performance, the concentrations increased steeply, showing the maximum values of 833 and 714 mg/L for the CDI and MCDI cells, respectively, when the desorption potential (0.0 V) was applied. Most ions were desorbed within 60 s after the application of the desorption potential. Because desorption proceed rapidly, it was easy to regenerate the electrode during the process operation.

As can be seen from Fig. 3, desalination occurred more effectively for the MCDI cell than for the CDI cell. It is noticeable that there is a significant difference in initial concentration changes for the two cell configurations. In the MCDI cell, the concentration of the effluent decreased sharply as the potential was applied, while the concentration increased and then decreased again for the CDI



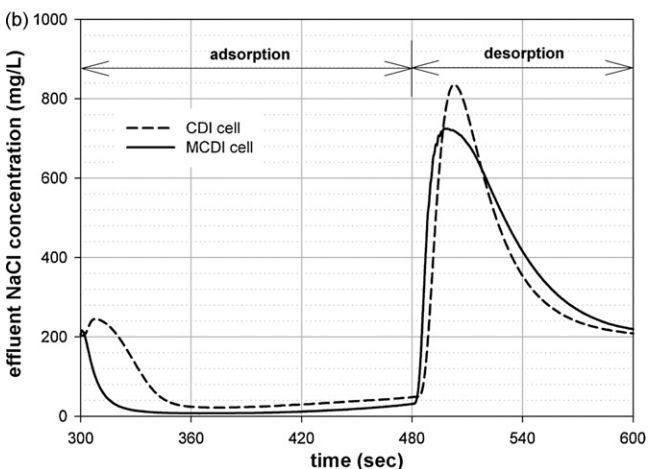


Fig. 3. (a) The NaCl concentration transient of effluent measured at a cell potential of 1.5 V with a flowrate of 20 mL/min and (b) the expanded concentration transient for the second cycle.

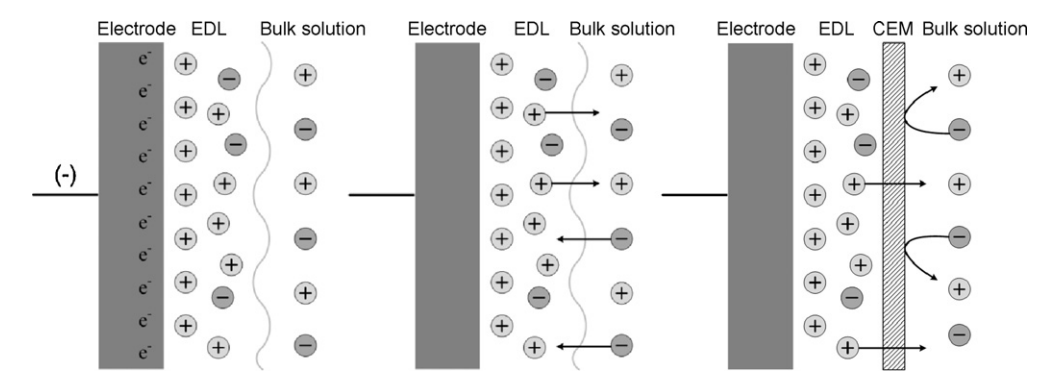


Fig. 4. The distribution and transport of ions at the electrode surface. Distribution of ions at the negatively charged electrode surface (a), and transport mechanism of ions when electrode potential is removed in the case without ion-exchange membrane (b), and with ion-exchange membrane (c).

cell; moreover, the rate of concentration decrease for the MCDI cell was greater than for the CDI cell.

These results could be explained through the adsorption and desorption mechanism of ions at the electrode surface. Fig. 4(a) shows the distribution of ions in the EDL when a negative potential was applied to the electrode. When the cell potential of 0.0 V was applied (Fig. 4(b)), the cations in the EDL moved to the bulk solution to re-establish electro-neutrality, which led to the desorption of ions; however, some anions could move from bulk solution to the EDL by electrostatic force. Accordingly, some amount of cations adsorbed at the electrode surface could not escape and were held in the EDL. In this situation, when the adsorption potential was reapplied to the electrode, the cations in the EDL were adsorbed onto the electrode surface. And anions expelled from the electrode simultaneously moved back to the bulk solution. This resulted in the slight uptick of effluent concentration at the beginning of adsorption period, as shown in Fig. 3 for the CDI cell.

Fig. 4(c) shows the transport of ions at the cathode combined with a cation-exchange membrane. In this case, the cations in the EDL could penetrate the cation-exchange membrane during the desorption process, but anions in bulk solution were rejected by the membrane. Accordingly, desalination efficiency was improved because of the selective transport of ions between the EDL and bulk solutions.

On the other hand, as shown in Fig. 3, the concentrations of the effluent increased sharply along with the desorption, which resulted in a four-fold increase in concentration. Most ions were desorbed within 1 min after the application of desorption potential.

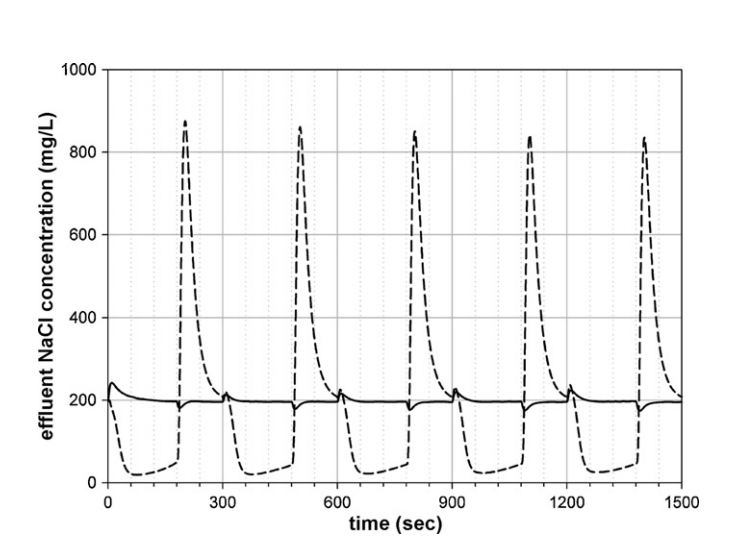


Fig. 5. The concentration transient of effluent measured at a cell potential of $-1.5\,\mathrm{V}$ with a flowrate of 20 mL/min. Solid line: MCDI cell, dashed line: CDI cell.

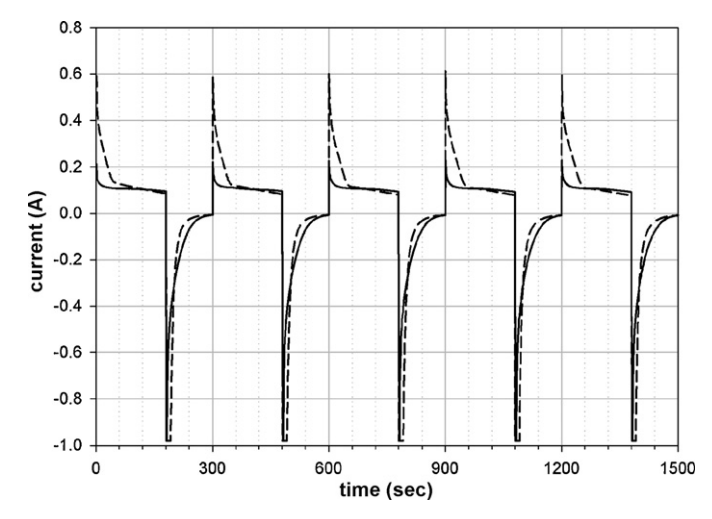


Fig. 6. The transient current flow through the cell at a potential of 1.5 V with a flowrate of 20 mL/min. Solid line: MCDI cell, dashed line: CDI cell.

Because the desorption proceeded rapidly, it was easy to regenerate the electrode during the process, meaning that it should be possible to increase the recovery ratio of the feed solution by reducing the desorption time.

In order to confirm the selectivity of the ion-exchange membrane, desalination experiments were carried out at the cell

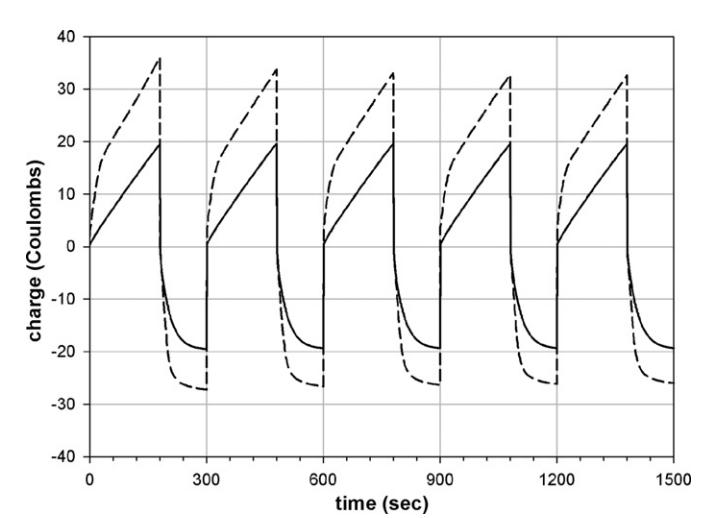


Fig. 7. The cumulative charges passed through the cell at a potential of 1.5 V with a flowrate of 20 mL/min. Solid line: MCDI cell, dashed line: CDI cell.

Table 1Comparison of salt removal efficiencies and the amount of salt removal for the CDI and MCDI cells at various operating conditions.

Operating conditions	Salt removal efficiency (%)		Amount of salt removal (mg NaCl/g of carbon)	
	CDI cell	MCDI cell	CDI cell	MCDI cell
1.2 V_20 mL/min	49.2	76.6	2.27	3.54
1.5 V_20 mL/min	62.5	83.0	2.88	3.83
1.5 V_30 mL/min	53.1	76.2	3.68	5.28

potential of $-1.5\,\mathrm{V}$ and the results are depicted in Fig. 5. As expected, the concentration changes for the CDI cell showed results similar to those with the cell potential at 1.5 V. Conversely, few ions were adsorbed and desorbed for the MCDI cell due to the rejection by the cation-exchange membrane. From these results, it was verified that the cation-exchange membrane on the cathode surface functioned well to transport ions selectively.

3.3. Current comparisons of the CDI and MCDI cell operations

Fig. 6 shows the changes in current transients supplied to the cell during five sorption—desorption cycles at 1.5 V adsorption potential and 0.0 V desorption potential, showing reproducible results for all cycles. For the CDI cell configuration, when a sorption potential was applied, the initial current of about 0.6 A rapidly decreased to around 0.1 A within 50 s and then continued to decrease gradually while about 0.1 A of current was supplied to the MCDI cell over the entire sorption period.

The current flow results provide further evidence of an ion-transport mechanism at the electrode surface. As described earlier, both anions and cations moved oppositely between the EDL and the bulk solution in the CDI cell configuration, which resulted in accumulation of ions in the EDL. When the voltage was applied to the electrodes again, ions in the EDL migrated to the electrode and to the bulk solution simultaneously. As a result, high currents are required to move these ions at the beginning of the adsorption period in the CDI cell configuration.

The desorption rate can be found indirectly from the current change. As soon as the desorption potential was applied, the currents fell to nearly zero within 1 min. This means that desorption of ions occurs very quickly. Compared with the CDI cell, it was observed that the desorption rate of MCDI cell was retarded due to the membrane resistance.

Fig. 7 shows the cumulative charges passed through the cell during the sorption and desorption periods. As expected from the transient current data, the charges increased linearly with increasing time for the MCDI cell, while in the CDI cell, a sudden increase of charges appeared at the beginning of the sorption period. The total charges supplied during the 3 min sorption period were measured at 32 and 20 C for the CDI and MCDI cells, respectively. Essentially similar charges were passed through the MCDI cell during desorption process, indicating that the sorption and desorption occurred mainly at the electrode surfaces due to the selective ion-exchange membrane in the MCDI cell configuration.

3.4. Comparison of salt removal efficiencies at various operating conditions

In order to compare the salt removal efficiencies related to the operating conditions for both cells, the electrosorption experiments were carried out at different cell potentials and flowrates. The effluents of adsorption and desorption period for each cycle were collected separately and the average NaCl concentration was measured to examine the amount of salt removed for each set of operating conditions. The salt removal efficiency, η_d , was calculated

according to the following equation [17]:

$$\eta_d(\%) = \left(1 - \frac{C_{eff}}{C_0}\right) \times 100 \tag{2}$$

where C_0 and C_{eff} are the influent and average NaCl concentrations of effluent during the adsorption period, respectively.

Table 1 shows the salt removal efficiencies and the amount of salt removal obtained at various operating conditions. Each of the CDI units tested exhibited increased salt removal with increased cell potential. Compared with the CDI cell, the MCDI cell exhibited a much better removal efficiency. For the case of a 1.5 V cell potential with a flowrate of 20 mL/min, the salt removal efficiencies of the CDI and MCDI cells were 62.5 and 83.0%, respectively. This shows that salt removal of the MCDI cell was 32.8% higher than that of the CDI cell. A high salt removal of 76.2% was recorded even for the flowrate of 30 mL/min in the MCDI cell configuration.

To compare the performances of the CDI and MCDI cells, the current efficiency was calculated. Current efficiency is defined as the ratio of ions adsorbed to the current passed through the cell and determined as following equation [29,30]:

$$\eta_{\text{current(\%)}} = \frac{(C_0 - C_{eff}) \cdot V \cdot F}{\int I dt} \times 100$$
 (3)

where V is volume of effluent, F is Faraday's constant and I is the current supplied.

Fig. 8 shows the current efficiencies obtained at various operating conditions for the CDI and MCDI cell configuration. In the CDI cell the current efficiencies were in the range of 35.5–43.1%, while the efficiencies increased to 83.8–91.3% for the MCDI cell. The higher current efficiency for the MCDI over the CDI cell was attributed to the selective adsorption and desorption in the MCDI cell configuration. According to the experimental results, it was concluded that introducing an ion-exchange membrane to the CDI cell as an ion-selective barrier was crucial to enhance the salt removal efficiency.

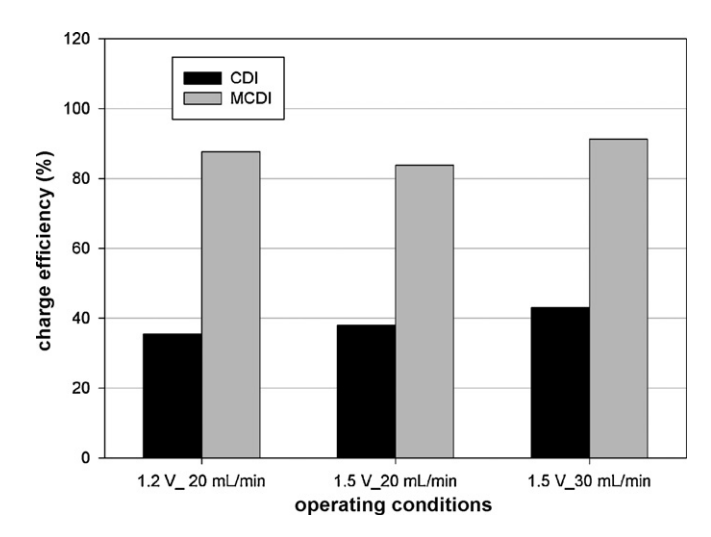


Fig. 8. Comparison of current efficiencies for the CDI and MCDI cells at various operating conditions.

4. Conclusions

Capacitive deionization has been regarded as a powerful deionization technology because of its advantageous features such as energy-efficiency and environmental friendliness. To enhance the salt removal efficiency of the CDI process, we investigated the adsorption and desorption mechanism on carbon electrode surfaces in this study.

Deionization experiments were carried out with two types of CDI cell configurations: a CDI cell with carbon electrodes only, and an MCDI including an ion-exchange membrane. The salt removal efficiencies of the MCDI cell were enhanced by about 32.8–55.9% compared to the CDI cell depending on the operating conditions. Furthermore, the current efficiencies were 35.5–43.1% for the CDI cell but 83.9–91.3% for the MCDI cell, about twice that of the CDI cell.

In the case of the CDI cell, some part of the ions was retained in the pore volume of the carbon electrode. Because these accumulated ions were re-adsorbed at the electrode surface when a potential was again applied, the salt removal efficiency and current efficiency were decreased in the CDI. Conversely, there was no accumulation of ions in the EDL for the MCDI cell due to the selective transport of ions by the ion-exchange membrane. It was concluded that introducing an ion-exchange membrane to the CDI cell as an ion-selective barrier was crucial to enhance the salt removal efficiency.

References

- [1] T. Younos, K.E. Tulou, J. Contemp. Water Res. Educ. 132 (2005) 3-10.
- [2] H. Strathmann, Ion-Exchange Membrane Separation Processes, Elsevier, Amsterdam 2004
- [3] L. Zou, L. Li, H. Song, G. Morris, Water Res. 42 (2008) 2340-2348.
- [4] L. Zou, G. Morris, D. Qi, Desalination 225 (2008) 329–340.

- [5] P. Xu, J.E. Drewes, D. Heil, G. Wang, Water Res. 42 (2008) 2605-2617.
- [6] J.C. Farmer, D.V. Fix, G.C. Mack, R.W. Pekala, J.F. Poco, J. Electrochem. Soc. 143 (1996) 159–169.
- [7] J.C. Farmer, D.V. Fix, G.C. Mack, R.W. Pekala, J.F. Poco, J. Appl. Electrochem. 26 (1996) 1007–1018.
- [8] C.J. Gabelich, T.D. Tran, I.H. Suffet, Environ. Sci. Technol. 36 (2002) 3010–3019.
- [9] K.C. Leonard, J.R. Genthe, J.L. Sanfilippo, W.A. Zeltner, M.A. Anderson, Electrochim. Acta 54 (2009) 5286–5291.
- [10] T.J. Welgemoed, C.F. Schutte, Desalination 183 (2005) 327-340.
- [11] J.A. Lim, N.S. Park, J.S. Park, J.H. Choi, Desalination 238 (2009) 37-42.
- [12] M.W. Ryoo, J.H. Kim, G. Seo, J. Colloid Interface Sci. 264 (2003) 414-419.
- [13] T.Y. Ying, K.L. Yang, S. Yiacoumi, C. Tsouris, J. Colloid Interface Sci. 250 (2002) 18–27.
- [14] K.K. Park, J.B. Lee, P.Y. Park, S.W. Yoon, J.S. Moon, H.M. Eum, C.W. Lee, Desalination 206 (2007) 86–91.
- [15] E. Ayranci, B.E. Conway, J. Electroanal. Chem. 513 (2001) 100-110.
- [16] Y. Gao, L. Pank, Y.P. Zhang, Y.W. Chen, Z. Sun, Surf. Rev. Lett. 14 (2007) 1033–1037.
- [17] H. Li, Y. Gao, L. Pan, Y. Zhang, Y. Chen, Z. Sun, Water Res. 42 (2008) 4923–4928
- [18] H.H. Jung, S.W. Hwang, S.H. Hyun, K.H. Lee, G.T. Kim, Desalination 216 (2007) 377–385.
- [19] C.H. Hou, C. Liang, S. Yiacoumi, S. Dai, G. Tsouris, J. Colloid Interface Sci. 302 (2006) 54–61.
- [20] K.L. Yang, T.Y. Ying, S. Yiacoumi, C. Tsouris, E.S. Vittoratos, Langmuir 17 (2001) 1961–1969.
- [21] R.W. Pekala, J.C. Farmer, C.T. Alviso, T.D. Tran, S.T. Mayer, J.M. Miller, B. Dunn, J. Non-Cryst. Solids 225 (1998) 74–80.
- [22] Y. Han, X. Quan, S. Chen, S. Wang, Y. Zhang, Electrochim. Acta 52 (2007) 3075–3081.
- [23] C.O. Ania, F. Béguin, Water Res. 41 (2007) 3372-3380.
- [24] M.D. Andelman, Charge barrier flow-through capacitor, CA Patent 2,444,390 (2002).
- [25] J.B. Lee, K.K. Park, H.M. Eum, C.W. Lee, Desalination 196 (2006) 125-134.
- [26] H. Pröbstle, M. Wiener, J. Fricke, J. Porous Mater. 10 (2003) 213-222.
- [27] H. Pröbstle, C. Schmitt, J. Fricke, J. Power Sources 105 (2002) 189-194.
- [28] R. de Levie, in: P. Delahay (Ed.), Advances in Electrochemistry and Electrochemical Engineering, vol. 6, Interscience, New York, 1967, p. 329.
- [29] K. Kinoshita, Carbon: Electrochemical and Physicochemical Properties, Wiley, New York. 1988.
- [30] B.E. Conway, Electrochemical Supercapacitors: Scientific Fundamentals and Technological Applications, Kluwer Academic/Plenum Publishers, New York, 1999.